Hot or not? An evaluation of methods for identifying hot moments of nitrous oxide emissions from soils

Emily R. Stuchiner[1,2,3,†], Jiacheng Xu[4], William C. Eddy[1,2,5], Evan H. DeLucia[1,2,5], Wendy H. Yang[1,2,5]

[1]Institute for Sustainability, Energy, and Environment, University of Illinois at Urbana-Champaign, Urbana, IL
[2]Agroecosystems Sustainability Center, University of Illinois at Urbana-Champaign, Urbana, IL
[3]Currently at Renewable and Sustainable Energy Institute, University of Colorado Boulder, CO
[4]Department of Statistics, University of Kentucky, Lexington, KY
[5]Department of Plant Biology, University of Illinois at Urbana-Champaign, Urbana, IL

Emily. R. Stuchiner: https://orcid.org/0000-0002-1567-0715
William C. Eddy: https://orcid.org/0000-0003-2215-9680
Evan H. DeLucia: https://orcid.org/0000-0003-3400-6286
Wendy H. Yang: https://orcid.org/0000-0002-2104-4796

[†]Corresponding author: Emily.Stuchiner@colorado.edu

Open access: We have uploaded all finalized data to www.scholar.colorado.edu Accession number forthcoming. In the meantime, data are available upon request.

Abstract

Effectively quantifying hot moments of nitrous oxide (N_2O) emissions from agricultural soils is critical for managing this potent greenhouse gas. However, we are challenged by a lack of standard approaches for identifying hot moments, including (1) determining thresholds above which emissions are considered hot moments, and (2) considering seasonal variation in the magnitude and frequency distribution of net N_2O fluxes. We used one year of hourly N_2O flux measurements from 16 autochambers that varied in flux magnitude and frequency distribution in a conventionally tilled maize field in central Illinois, USA to compare three approaches to identify hot moment thresholds: 4x the standard deviation (SD) above the mean, 1.5x the interquartile range (IQR), and isolation forest (IF) identification of anomalous values. We also compared these approaches on seasonally subdivided data (early, late, non-growing seasons) vs. the whole year. Our analyses of the datasets revealed that 1.5x IQR method best identified N_2O hot moments. In contrast, the 4 SD method yielded hot moment threshold values too high, and the IF method yielded threshold values too low, leading to missed N_2O hot moments or low net N_2O fluxes mischaracterized as hot moments, respectively. Furthermore, seasonally subdividing the dataset facilitated identification of smaller hot moments in the late and non-growing seasons when N_2O hot moments were generally smaller, but it also increased hot moment threshold values in the early growing season when N_2O hot moments were larger. Consequently, we recommend using the 1.5x IQR method on whole year datasets to identify N_2O hot moments.

Plain Language Summary

Nitrous oxide (N_2O) is a greenhouse gas that traps 273 times more heat in Earth's atmosphere than carbon dioxide (CO_2) on a per molecule basis. Microbes in the soil produce N_2O, with short bursts of high production stimulated by environmental triggers such as rainfall or fertilization. Management strategies targeting these brief periods of high N_2O production can be particularly effective in reducing cumulative annual soil N_2O emissions from agricultural fields. However, to date there is no standard approach to identifying hot moments. Here, we analyzed 16 one-year datasets of hourly N_2O emission measurements from a large area in one maize field to compared different methods that are used to identify hot moments of N_2O. We learned that the threshold values above which N_2O emissions would be considered hot moments were best determined as 1.5 times greater than the N_2O emission value that fell in the middle of all the emission values in the dataset, a method called "1.5x the interquartile range." We could also best identify hot moments of N_2O when we analyzed the whole year N_2O datasets as opposed to seasonally subdividing the datasets. Our recommendations to standardize N_2O hot moment identification will facilitate synthesis of knowledge across studies.

Introduction

Nitrous oxide (N_2O) currently accounts for 6% of Earth's radiative forcing (Dutton et al. 2023), and soil emissions contribute significantly to rising atmospheric concentrations of this potent greenhouse gas. Soil N_2O emissions are often characterized by short periods of high reaction rates that contribute disproportionately to cumulative annual N_2O emissions, referred to as hot moments (Groffman et al. 2009, Bernhart et al. 2015, Wagner-Riddle et al. 2020). Hot moments are prime targets for land management practices to mitigate N_2O emissions, especially in agroecosystems (Wagner-Riddle et al. 2020). However, there is high uncertainty in the effectiveness of agricultural land management practices in reducing emissions, in part because assessments largely rely on relatively infrequent manual chamber-based emissions measurements that may miss many of the hot moments (Kravchenko and Robertson 2015, Charteris et al. 2020). Understanding of N_2O hot moments from high temporal resolution datasets derived from autochamber and micrometeorological measurements can help guide improved manual chamber measurement sampling to better capture hot moments (Tallec et al. 2019, Lawrence et al. 2021, Anthony and Silver 2021) and parameterize models to more accurately predict N_2O budgets on regional to global scales (O'Connell et al. 2022). Despite these datasets becoming more common (Charteris et al. 2020, Dorrich et al. 2020), there currently is no standard approach for hot moment identification, and the implications of different approaches on hot moment identification and quantification have not previously been evaluated.

There are several methods for identifying N_2O hot moments, wherein emission values above a threshold are considered part of an N_2O hot moment (Bernhart et al. 2015). Often, thresholds are arbitrarily determined when visualizing the time series of net N_2O flux data (Mander et al. 2021, Rautakoski et al. 2023). Statistical methods can be applied in a more standardized manner across studies, but the threshold values determined depend on the frequency distribution of individual N_2O flux datasets. For example, assuming a dataset is normally distributed, using 1.5x the interquartile range (1.5x IQR; e.g., Molodovskaya et al. 2012) of the measured net N_2O fluxes, flux values higher than 99.3% of the distribution are considered part of N_2O hot moments. Using four standard deviations (4 SD) above the mean (e.g., Anthony and

Silver 2021), only flux values in the top 0.1% of the distribution are identified as hot moments. These statistical methods are grounded in the assumption that datasets are normally distributed; however, this assumption belies the very behavior of N_2O hot moments (episodic and large emission pulses), which typically leads to right skewed N_2O flux datasets. Transforming the datasets to achieve normal distributions can lead to extremely high threshold values that result in few identified hot moments, particularly using the 4 SD method. Consequently, distribution-free methods such as isolation forest (IF) classification, which are free of assumptions about the shape of the probability distribution of a dataset, could be more appropriate for hot moment identification (Ackett et al. 2022). Isolation forest (IF) classification is a machine-learning method that uses binary trees to identify anomalous data points based on short path-lengths in the trees that indicate that the data points are few and different from the rest of the dataset. These threshold determination methods have not been compared across N_2O flux datasets that vary in flux magnitude and distribution, leaving uncertain how much the methods can differ in hot moment identification and the estimated fraction of annual N_2O emissions attributed to hot moments.

Seasonal variation in N_2O flux magnitude and distribution could lead to bias in hot moment identification and quantification when considering whole year datasets compared to seasonally subdivided datasets. In agroecosystems, N_2O hot moments are largely governed by seasonally distinct triggers (Butterbach-Bahl et al. 2013). In the early growing season fertilization with ammonium (NH_4^+) or nitrate (NO_3^-) drives hot moments (Molodovskaya et al. 2012, Roy et al. 2014). Throughout the growing season, irrigation or rainfall drives hot moments (Griffis et al. 2017, Song et al. 2021). During the winter and spring, freeze-thaw and thaw drive hot moments, respectively (Risk et al. 2013, Wagner-Riddle et al. 2017). The flux magnitudes of these hot moments vary, with fertilization-driven hot moments typically yielding larger-magnitude N_2O fluxes than rainfall-driven hot moments (Kostyanovsky et al. 2019). Thaw-related hot moments can be even larger but vary in magnitude depending on the strength of a freeze event prior to thaw (Butterbach-Bahl et al. 2002, Groffman et al. 2009). Mitigating both larger and smaller N_2O hot moments can potentially be important to reducing annual N_2O emissions, with mitigation strategies targeting the different mechanisms responsible for N_2O hot moments in different seasons. However, studies to date have conducted hot moment identification on whole year datasets such that the larger fertilization and thaw-driven N_2O emission pulses elevate the thresholds used to identify N_2O hot moments, causing the smaller, more frequent hot moments from other seasons to be missed. Because seasonally subdivided hot moment identification has not been previously conducted, it is not known how much these smaller N_2O hot moments contribute to annual N_2O emissions.

Here, we evaluated different threshold determination methods on whole year and seasonally subdivided net N_2O flux datasets to determine which approach best captured N_2O hot moments across datasets varying in N_2O flux magnitude and distribution. We took advantage of a unique study in which one year of hourly measurements of net N_2O flux were collected from 16 autochambers located in a ~5 ha area of a conventionally tilled maize field in central Illinois, USA. The autochambers were placed to capture variation in N_2O dynamics, including consistent N_2O cold spots and episodic N_2O hot spots (Zhang et al. 2023). The variation in N_2O flux magnitude and distribution among the 16 autochamber datasets provided the opportunity to robustly assess how hot moment identification using (1) the 4 SD, 1.5x IQR and IF methods, and (2) whole year datasets versus seasonally subdivided datasets (early growing season, late growing season, and non-growing season) affected hot moment threshold values and quantification of N_2O hot moment fluxes. Based on our findings, we provide recommendations to standardize hot moment identification approaches.

Methods

Net N_2O flux data collection

Net N_2O fluxes were measured in a commercial field located near Villa Grove, IL that was cultivated in maize-maize-soy rotations with conventional tillage and planted with maize (*Z. mays*) during the 2022 growing season. Deep chisel tillage was performed in November 2021. Pre-planting fertilizers were applied at the rate of 19.7 kg N ha^{-1}, 93.1 kg P ha^{-1}, and 53.8 kg K ha^{-1} in April 2022. Prior to planting, 134.5 kg N ha^{-1} of anhydrous ammonia was injected into the soil on May 7, 2022. Maize was planted on May 10, 2022. Finally, 32% UAN was Y-dropped as side-dressing at 90.2 kg N ha^{-1} with ammonium thiosulfate at 13.2 kg N ha^{-1} on June 11, 2022. *Z. mays* was harvested on October 28, 2022. The soil in the field is roughly 70% Drummer silty clay loam and 30% Millbrook silt loam (USDA-NRCS, 2022). In this region, the mean annual air temperature is 10 °C, with a maximum monthly mean temperature of 24.4 °C in July and a minimum of -5.5 °C in January (Midwestern Regional Climate Center). The mean annual precipitation is 1008 mm, of which most rainfalls occur during the period of May to July (Illinois-Climate-Network, 2017).

To capture spatial and temporal variability in soil N_2O emissions at the field scale, net soil-atmosphere fluxes of N_2O were measured hourly using automated chambers at 16 locations in the maize field. The chambers were distributed among four sampling nodes within a ~5 ha area of the field. At each node, four automated chambers (LI-8200-104, LI-COR Biosciences, Lincoln, NE, USA) were radially installed at 12 m distance from a N_2O gas analyzer (LI-7820, LI-COR Biosciences, Lincoln, NE, USA) that sequentially measured hourly net soil-atmosphere N_2O fluxes from each chamber continuously with an automated gas sampling multiplexer (LI-8250, LI-COR Biosciences, Lincoln, NE, USA) starting in May 2022 until April 2023, excluding a ~3-week period in October-November 2022 during crop harvest.

Comparison of hot moment identification approaches

We compared three threshold value determination methods (4 SD, 1.5x IQR, and IF) on whole year datasets and seasonally subdivided datasets to determine how the hot moment identification approaches affected the hot moment threshold values, the percentage of hot moment contributions to annual or seasonal N_2O emissions, and the percentage of time in the year or season attributed to hot moments. The year was divided into three seasons: the early growing season (May 13-July 7, 2022) when hot moments were driven by fertilizer inputs, the late growing season (July 8-October 30, 2022) when hot moments were driven by rain events, and the non-growing season when hot moments were driven by freeze-thaw events (November 1, 2022-April 9, 2023). The breakpoints between the seasons were visually determined from plotting the whole year datasets for the 16 autochambers together (Figure S1).

We ran each of the threshold value determination methods for the whole year and by individual season for each of the 16 autochambers. For the 4 SD method, we calculated the mean and SD of the dataset and then determined the hot moment threshold value as four SD above the mean. For the 1.5x IQR method, the IQR is calculated as the difference between the 75th percentile (Q3) and the 25th percentile (Q1) of the dataset. To identify the hot moment threshold, we calculated the upper threshold, which is Q3 plus 1.5 times the IQR. The IF method isolates anomalies instead of profiling normal data points. The algorithm utilizes 'isolation trees' to partition the data space, where anomalies are identified based on shorter path lengths in these trees, indicating easier isolation compared to normal points. For IF, we employed the IsolationForest function from sklearn.ensemble module in Python (version 3.10), setting the contamination parameter to 'auto'. This configuration allows the algorithm to automatically estimate the proportion of outliers in the dataset. This approach classifies data points with an anomaly score below 0 as anomalies. The threshold for identifying significant hot moments in N_2O flux was determined by the lowest net N_2O flux value that corresponded to an anomaly score below this threshold.

Although all 16 autochamber datasets were right-skewed (Figure S2), for several reasons we chose not to transform the datasets to achieve normal distributions. First, about 4% of the net N_2O flux measurements across all datasets were negative fluxes that would have to be excluded to proceed with log transformation. Second, log transformation would diminish the data points on the high end of the frequency distributions such that the hot moment identification methods would not capture these extreme values as “hot moments.” Third, IF is an unsupervised learning algorithm that does not assume a specific distribution, negating the need for transformation.

Using the determined threshold values above which a data point was considered part of a hot moment, we calculated the cumulative hot moment N_2O emissions and the number of hot moment data points. We calculated the percentage of hot moment contributions to cumulative N_2O emissions from the cumulative hot moment N_2O emissions divided by cumulative N_2O emissions. We also calculated the percentage of time in hot moments from the number of hot moment data points divided by the total number of N_2O flux data points. These calculations were performed separately for each of the 16 autochambers across the whole year and by individual season.

Statistical analyses

We used one-way ANOVAs and Tukey pairwise comparisons to determine the effect of threshold determination method on threshold values, percentage of hot moment contributions to the cumulative N_2O emissions, and the percentage of time in hot moments in the whole year and in individual seasons. We also conducted similar analyses within each threshold determination method to determine the effect of season. Additionally, we calculated Pearson's coefficient of skew using the median for each autochamber's N_2O flux measurements. The 16 autochambers were considered independent replicates for this analysis because of the high variation among autochamber datasets, even within sampling nodes. This analysis was performed separately for the whole year datasets and for each of the three individual season datasets. These statistical analyses were performed in RStudio (version 4.2.2 (2022-10-31) -- "Innocent and Trusting" © 2022 The R Foundation for Statistical Computing). Statistical significance was determined as $P < 0.05$.

Results

Comparison of hot moment threshold values

On average across all 16 autochamber datasets, the 4 SD method yielded 1-2 orders of magnitude higher threshold values compared to the 1.5x IQR and IF methods, which had comparably lower threshold values (Table 1). The 4 SD method threshold values were significantly higher than the other two methods when considering the whole year and individual seasons (Table 1). This difference was detectable despite high variation in threshold values among autochambers: for the whole year analysis, thresholds ranged from 0.39-2.2, 0.0002-2.2, and 3.7-36 nmol N_2O m^{-2} s^{-1} for 1.5x IQR, IF, and 4 SD methods, respectively (Figure S3).

When subdividing the datasets into the early, late, and non-growing seasons, the threshold values determined by a given threshold determination method differed significantly among seasons (Table 1, Figure S3). All three methods yielded higher threshold values in the early growing season compared to the other two seasons, although for the IF method this was not statistically significant for the early versus non-growing season comparison (Table 1, Figure S4). Seasonally subdividing the datasets led to increased early growing season hot moment thresholds compared to whole year thresholds for the 1.5x IQR and 4 SD methods, whereas it did not significantly decrease the late- and non-growing season thresholds relative to the whole year thresholds. In contrast, seasonally subdividing the datasets led to decreased late- and non-growing season thresholds compared to whole year thresholds for the IF method, and it did not change the early season threshold relative to the whole year threshold.

Table 1. Mean ± SE net N_2O flux threshold values (nmol N_2O m^{-2} s^{-1}) for the three hot moment threshold determination method applied to whole year datasets and seasonally subdivided datasets (N = 16 in all cases). Different lowercase letters indicate statistically significant Tukey pairwise differences at $P < 0.05$ among the threshold determination methods. Different uppercase letters indicate statistically significant Tukey pairwise differences at $P < 0.05$ among the time intervals for each threshold determination method. The column of ANOVA main effects corresponds to the differences among threshold determination methods, and the row of ANOVA main effects corresponds to the differences among seasons for a given method. For all one-way ANOVAs, df = 2. For $P < 0.001$, ***; $P < 0.01$ **; $P < 0.05$, *. To see all threshold values for each autochamber by method and season, see Figures S3 and S4 in the Supplement.

	Threshold determination method			**Compare by method**
	1.5x IQR	Isolation forest	4 SD	ANOVA main effects
Time interval				
Whole year	1.5 ± 0.24 (**a, A**)	0.89 ± 0.14 (**a, B**)	9.9 ± 2.0 (**b, AB**)	P < 0.001, F = 18 ***
Early growing season	5.0 ± 0.90 (**a, B**)	0.92 ± 0.36 (**a, B**)	19 ± 4.6 (**b, B**)	P < 0.001, F = 12 ***
Late growing season	1.3 ± 0.44 (**a, A**)	0.07 ± 0.03 (**a, A**)	3.9 ± 0.83 (**b, A**)	P < 0.001, F = 12 ***
Non-growing season	0.91 ± 0.28 (**a, A**)	0.34 ± 0.07 (**a, AB**)	2.7 ± 0.66 (**b, A**)	P < 0.001, F = 8.4 ***
Compare by time interval				
ANOVA main effects	P <0.001, F = 13 ***	P = 0.01, F = 4.6 *	P < 0.001, F = 8.1 ***	

Comparison of hot moment contributions to cumulative N_2O emissions

For the whole year and each season, the percentage of cumulative N_2O emissions from each chamber that was attributed to hot moments was, on average, lowest for the 4 SD method compared to the other two threshold determination methods (Table 2). However, this pattern did not necessarily hold when comparing the three methods for a given chamber within an individual season (Figure 1). In the early growing season, the three methods were sometimes indistinguishable. For example, regardless of the threshold determination method, 99-100% of the cumulative seasonal N_2O emissions was attributed to hot moments for the five autochambers with the highest cumulative early season N_2O emissions (N1C3, N1C4, N4C1, N4C2, N4C3; Figure 1). For one chamber (N3C2), the IF method attributed 100% of cumulative seasonal N_2O emissions to hot moments in all three seasons, which was far higher than the other two methods.

For all threshold determination methods, the mean percentage of cumulative seasonal N_2O emissions attributed to hot moments was greater in the early growing season compared to the late and non-growing seasons (Table 2). However, this pattern did not necessarily hold across all chambers (Figure 1). For example, in Node 2, for Chambers 1 and 3, most of the cumulative annual flux was attributed to the non-growing season, but for Chambers 2 and 4 the cumulative N_2O flux is more evenly distributed among the seasons (Figure 1).

The percentage of time attributed to hot moments was higher for whole year datasets compared to the sum of seasonally subdivided datasets for the 1.5x IQR and 4 SD methods but was the opposite for the IF method (Table 2). The hot moment contributions for 1.5x IQR, IF, and 4 SD differed by 19%, 9%, and 12%, respectively, for the summed seasonal contributions vs. the whole year contributions (Table 2). Chamber by chamber, there was some more notable variation between the two approaches, but not across all chambers. Chambers that varied by 20%

or more between the seasonally summed vs. whole year hot moment contributions included: all Node 1 chambers, N3C1, and N4C3 for 1.5x IQR, N2C2, N2C4, and N4C4 for IF, and N4C1 and N4C2 for 4 SD (Figure S5).

Table 2. Mean ± SE hot moment contribution percentages (%) for the three hot moment threshold determination methods applied to whole year datasets and seasonal datasets (n = 16 in all cases). Different lowercase letters indicate statistically significant Tukey pairwise differences at $P < 0.05$ among the threshold determination methods. Different uppercase letters indicate statistically significant Tukey pairwise differences at $P < 0.05$ among the time intervals for each threshold determination method. The column of ANOVA main effects corresponds to the differences among threshold determination methods, and the first row of ANOVA main effects corresponds to the differences among seasons within a method. The second row of ANOVA main effects corresponds to the differences between the whole year versus the sum of individual seasons. For all one-way ANOVAs, df = 2. For $P < 0.001$, ***, $P < 0.01$ **, $P < 0.05$, *.

	Threshold determination method			**Compare by method**
	1.5x IQR	Isolation forest	4 SD	ANOVA main effects
Time interval				
Whole year	66 ± 2.8 (**b, AB**)	76 ± 2.9 (**a, A**)	24 ± 2.3 (**c, A**)	P < 0.001, F = 107 ***
Early growing season	85 ± 6.1 (**ab, B**)	96 ± 1.8 (**b, B**)	65 ± 8.2 (**a, B**)	P = 0.003, F = 6.7 **
Late growing season	57 ± 9.4 (**ab, A**)	72 ± 8.0 (**b, A**)	37 ± 8.8 (**a, A**)	P = 0.03, F = 4.0 *
Non-growing season	48 ± 3.9 (**b, A**)	70 ± 3.3 (**c, A**)	16 ± 1.8 (**a, A**)	P < 0.001, F = 76 ***
All seasons summed	47 ± 3.5 (**b, A**)	87 ± 3.0 (**c, B**)	12 ± 2.3 (**a, A**)	P < 0.001, F = 177 ***
Compare by time interval				
ANOVA main effects	P < 0.001, F = 6.7 ***	P < 0.001, F = 6.6 **	P < 0.001, F = 12 ***	
	P < 0.001, F = 18 ***	P = 0.02, F = 6.2 *	P < 0.001, F = 16 ***	

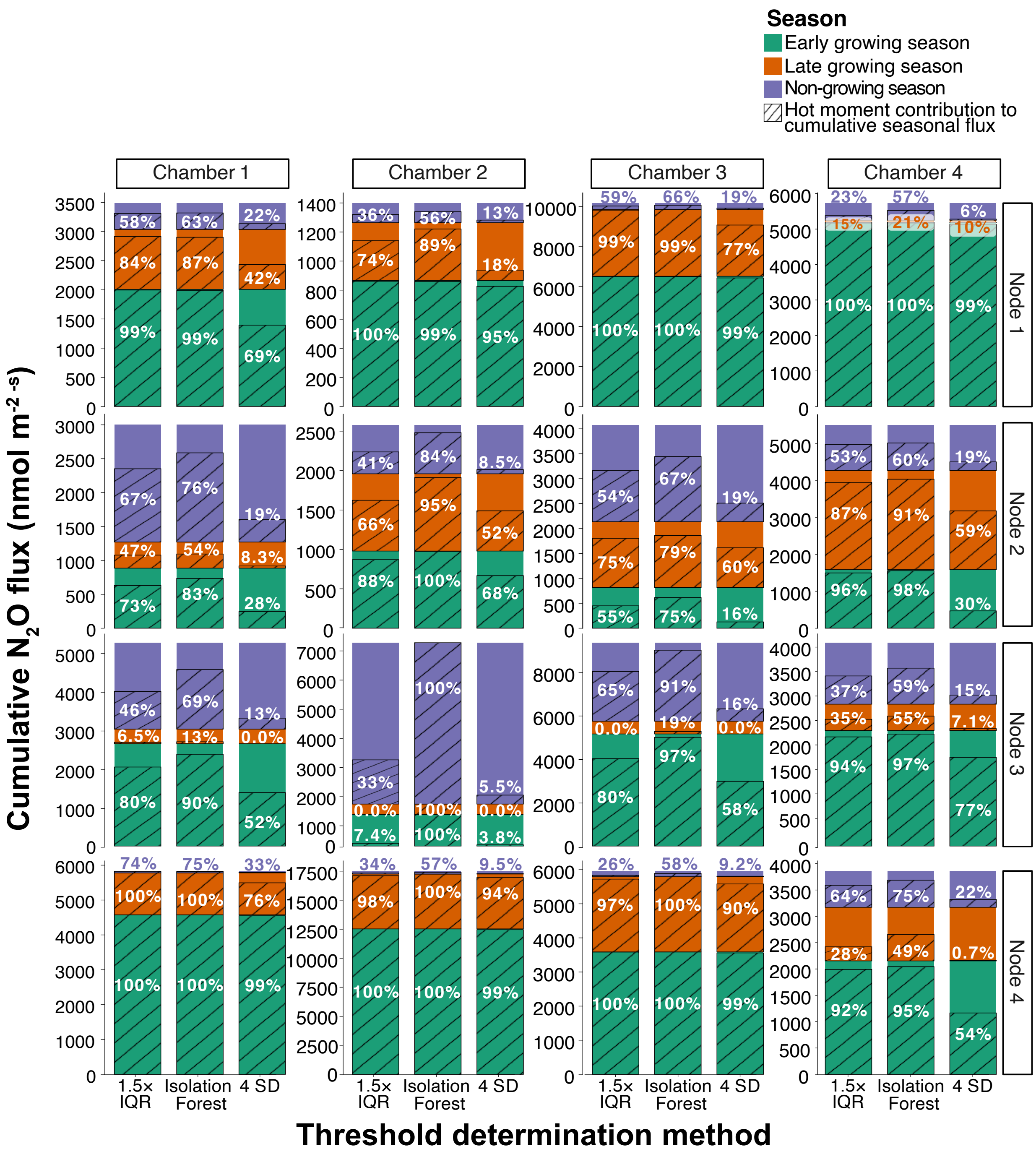

Figure 1. Hot moment contributions to the cumulative N_2O flux for each automated chamber over the whole sampling period (May 2022-April 2023). For each automated chamber (each panel in the figure), the three bars correspond to the three threshold determination methods, the different color portions within each bar correspond to a different season, and the shaded fraction of each colored portion corresponds to the N_2O flux values that were included in hot moments. Flux values greater than or equal to the threshold value were considered part of a hot moment. The percentage values written inside each colored bar portion corresponds to the percentage of the N_2O flux for each season that was attributed to hot moments of N_2O.

Comparison of the amount of time attributed to hot moments

The percentage of time within each season attributed to hot moments was significantly lower for the 4 SD and 1.5x IQR methods compared to the IF threshold determination method (Table 3, Figure S6). Within each season, roughly 1% and 9% of data points were categorized as hot moments by the 4 SD and 1.5x IQR methods, respectively. Among seasons, the 1.5x IQR and 4 SD methods attributed similar percentages of time to hot moments. In contrast, on average across all 16 autochambers, the IF method led to a highly variable percentage of time attributed to hot moments, ranging from 23% in the non-growing season to 89% in the late growing season. In addition, IF attributed higher percentages of time to hot moments during the early and late growing seasons, but a much lower percentage of time to hot moments during the non-growing season (Table 3, Figure S6).

Table 3. Mean percentage of time for each season that was identified as a hot moment using the different threshold determination methods, averaged across all chambers (n = 16 in all cases); ± corresponds to 1 SE from the mean, and letters correspond to Tukey pairwise differences. Different lowercase letters indicate statistically significant Tukey pairwise differences at $P < 0.05$ among the threshold determination methods. Different uppercase letters indicate statistically significant Tukey pairwise differences at $P < 0.05$ among the seasons for each threshold determination method. The column of ANOVA main effects corresponds to the differences among threshold determination methods, and the row of ANOVA main effects corresponds to the differences among seasons within a method. For all one-way ANOVAs, df = 2. For $P < 0.001$, ***, $P < 0.01$ **, $P < 0.05$, *.

	Threshold determination method			**Compare by method**
	1.5x IQR	Isolation forest	4 SD	ANOVA main effects
Season				
Early growing season	9.3 ± 1.0 (**a, A**)	65 ± 9.7 (**b, B**)	0.81 ± 0.11 (**a, A**)	P < 0.001, F = 38 ***
Late growing season	7.7 ± 1.2 (**b, A**)	89 ± 7.2 (**a, B**)	0.85 ± 0.15 (**b, A**)	P < 0.001, F = 136 ***
Non-growing season	8.8 ± 0.58 (**a, A**)	23 ± 5.3 (**b, A**)	1.2 ± 0.07 (**a, A**)	P < 0.001, F = 13 ***
Compare by season				
ANOVA main effects	P = 0.51, F = 0.70	P < 0.001, F = 19 ***	P = 0.08, F = 2.7	

Discussion

To better measure and mitigate N_2O emissions, we must identify and quantify hot moments of N_2O that contribute disproportionately to annual N_2O budgets. Currently, there is no standard approach for hot moment identification, which challenges synthesis of knowledge about N_2O hot moments across studies. The work we present here is the first assessment of different approaches for hot moment identification and their implications for hot moment quantification.

Our analysis of 16 hourly net N_2O flux datasets that vary in N_2O flux magnitude and distribution revealed that the 4 SD method yielded hot moment threshold values too high, and the IF method yielded threshold values too low. This led to missed N_2O hot moments or low net N_2O fluxes mischaracterized as hot moments, respectively (Table 1, Figure S3, Figure 1). Hot moment identification by the 1.5x IQR method was most consistent with the definition of N_2O hot moments, yielding an estimate that on average 9% of the net N_2O fluxes measured over the year were hot moments that contributed 66% of the cumulative N_2O emissions (Table 3, Table 2). Seasonally subdividing the annual datasets facilitated identification of smaller hot moments in the late and non-growing seasons when N_2O hot moments were generally smaller (Table 2, Figure S4, Figure 1). However, it also increased the 4 SD and 1.5x IQR hot moment threshold values in the early growing season when N_2O hot moments were larger, leading to lower estimates of hot moment contributions to annual N_2O emissions (Table 1, Figure S5). In the interest of identifying the N_2O hot moments that are most important to measure and mitigate, we recommend whole year analyses as opposed to seasonally subdivided analyses.

Evaluation of hot moment threshold determination methods

Our analysis suggests that the 4 SD method was too stringent for hot moment identification, missing what would reasonably be considered hot moments in visual evaluations of the 16 autochamber datasets (Figure S7). By definition, this method should only identify the top 0.1% of the net N_2O flux data as hot moments in datasets exhibiting normal distributions. When we applied the 4 SD method to untransformed right-skewed datasets, approximately 1% of the net N_2O flux data were identified as hot moments (Table 3). On average across the 16 autochamber datasets, the 4 SD method yielded ten times higher hot moment threshold values which led to three times lower estimates of hot moment contributions to annual N_2O emissions compared to the 1.5x IQR and IF methods (Table 1, Figure 1). The high threshold values estimated by the 4 SD method not only caused smaller hot moments to be missed but also caused net N_2O fluxes on the rising and falling limbs of large hot moment pulses to be missed (Figure S7). An exception to this stark difference between methods was the autochamber datasets that included extremely high N_2O fluxes following fertilization, which led to comparably high early growing season hot moment contributions (99-100%) estimated by all three methods (Figure 1, Table 2). Our analysis suggests that the 4 SD method would not capture the importance of the smaller-magnitude hot moments to cumulative annual N_2O budgets. We conclude that the 4 SD method is appropriate for identifying the hottest hot moments that are most important to measure and mitigate (Anthony and Silver 2021), but it is likely not ideal for developing comprehensive models of annual N_2O flux patterns because it only effectively hones in on the greatest hot moment triggers.

The 1.5x IQR and IF methods yielded similar estimates of hot moment contributions to annual or seasonal N_2O emissions (Figure 1, Figure S5), but the IF method often attributed considerably more net N_2O flux data to hot moments (Figure S6, Table 3). This was due to lower hot moment threshold values estimated by the IF method which led to more N_2O flux data points attributed to hot moments (Table 1, Figure S3). However, these smaller "N_2O hot moments" contributed little to cumulative N_2O emissions over the year or the individual season (Figure S3, Figure S4, Figure 1). This was most exaggerated in the late growing season, which was marked by few and small hot moments across most autochambers. On average across the 16 autochamber datasets, the late growing season threshold value estimated by the IF method was so low (ten times lower than that estimated by the 1.5x IQR method), that 89% of late growing season net N_2O flux data points were attributed to hot moments (Figure S4, Table 2). Even in the early growing season when large hot moments occurred, the IF method on average attributed 65% of net N_2O flux data points to hot moments (Table 2). The IF method, therefore, appears too permissive in identifying N_2O hot moments which should represent short periods of high net N_2O fluxes that disproportionately contribute to cumulative N_2O emissions (Wagner-Riddle et al. 2020). In contrast, the percentage of net N_2O fluxes attributed to hot moments by the 1.5x IQR method was constrained to ~9%, which is more in line with the definition of hot moments (Table 3, Figure S6; Wagner-Riddle et al. 2020). We conclude that, of the three threshold determination methods we evaluated, the 1.5x IQR method strikes the best balance in identifying hot moments. Moreover, although there are not yet many published studies that have analyzed high temporal resolution N_2O flux measurements for hot moments, a substantial fraction of published studies have opted to use the 1.5x IQR method (e.g., van den Heuvel et al. 2009, Molodovskaya et al. 2012, Li et al. 2015, Bastos et al. 2021), likely because it can robustly detect hot moments even when they vary in flux magnitude.

Evaluation of whole year versus seasonally subdivided analyses

Because different mechanisms trigger different magnitude N_2O hot moments in the different seasons, we evaluated seasonally subdivided N_2O flux datasets to ensure that hot moments were appropriately identified in all seasons. While most of the 16 autochamber datasets exhibited large N_2O hot moments in the early growing season and smaller N_2O hot moments in the late- and non-growing seasons (Figure 1, Figure S7), the threshold values estimated from the analysis of whole year datasets did not exclude the smaller N_2O hot moments (Table 1). As such, seasonally subdividing the datasets was not necessary to improve hot moment identification. On the contrary, it detrimentally affected hot moment identification in the early growing season by raising the hot moment threshold value estimated by the 4 SD and 1.5x IQR methods (Table 1). This resulted in a decrease in estimated hot moment contributions to annual N_2O emissions (Figure 1, Table 2). For the IF method, the low threshold values estimated for the late and non-growing seasons led to more than half of those seasons being inappropriately identified as hot moments, thereby increasing the estimated hot moment contribution to annual N_2O emissions relative to whole year analysis (Figure 1). We conclude that seasonal subdivision of N_2O flux datasets can be counterproductive to N_2O hot moment identification and quantification regardless of the threshold determination method.

Data Availability Statement

We have uploaded all finalized data to www.scholar.colorado.edu Accession number forthcoming.

Prepublication note: These data are embargoed, pending publication of this manuscript.

Acknowledgements: We appreciate assistance in the laboratory and field by Ava Bernacchi, Ally Cook, Ingrid Holstrom, Neiman Shivers, Haley Ware, and Chloe Yates.

Funding: This study was supported by the U.S. Department of Energy ARPA-E SMARTFARM program under Award Number DE-AR0001382.

Competing interests: The authors have no relevant financial or non-financial interests to disclose.

Works Cited

1. Ackett, R., Saha, D., Gelfand, I., & Hilafu, H. (2022, November). Predicting Agricultural Nitrous Oxide "Hot Moment" Occurrences and Drivers Using Machine Learning Techniques. In *ASA, CSSA, SSSA International Annual Meeting*. ASA-CSSA-SSSA.

2. Anthony, T. L., & Silver, W. L. (2021). Hot moments drive extreme nitrous oxide and methane emissions from agricultural peatlands. *Global change biology*, *27*(20), 5141-5153.

3. Bastos, L. M., Rice, C. W., Tomlinson, P. J., & Mengel, D. (2021). Untangling soil-weather drivers of daily N2O emissions and fertilizer management mitigation strategies in no-till corn. *Soil Science Society of America Journal*, *85*(5), 1437-1447.

4. Bernhardt, E. S., Blaszczak, J. R., Ficken, C. D., Fork, M. L., Kaiser, K. E., & Seybold, E. C. (2017). Control points in ecosystems: moving beyond the hot spot hot moment concept. *Ecosystems*, *20*, 665-682.

5. Butterbach-Bahl, K., Rothe, A., & Papen, H. (2002). Effect of tree distance on N 2 O and CH 4-fluxes from soils in temperate forest ecosystems. *Plant and Soil*, *240*, 91-103.

6. Butterbach-Bahl, K., Baggs, E. M., Dannenmann, M., Kiese, R., & Zechmeister-Boltenstern, S. (2013). Nitrous oxide emissions from soils: how well do we understand the processes and their controls?. *Philosophical Transactions of the Royal Society B: Biological Sciences*, *368*(1621), 20130122.

7. Charteris, A. F., Chadwick, D. R., Thorman, R. E., Vallejo, A., de Klein, C. A., Rochette, P., & Cárdenas, L. M. (2020). Global Research Alliance N2O chamber methodology guidelines: Recommendations for deployment and accounting for sources of variability. Journal of Environmental Quality, 49(5), 1092-1109.

8. Dutton GS, Hall BD, Dlugokencky EJ, Lan X, Nance JD, Madronich M. Combined atmospheric nitrous oxide dry air mole fractions from the NOAA GML halocarbons sampling network, 1977-2023, Version: 2023-04-13 (2023).

9. Griffis, T. J., Chen, Z., Baker, J. M., Wood, J. D., Millet, D. B., Lee, X., ... & Turner, P. A. (2017). Nitrous oxide emissions are enhanced in a warmer and wetter world. *Proceedings of the National Academy of Sciences*, *114*(45), 12081-12085.

10. Groffman, P. M., Butterbach-Bahl, K., Fulweiler, R. W., Gold, A. J., Morse, J. L., Stander, E. K., ... & Vidon, P. (2009). Challenges to incorporating spatially and temporally explicit phenomena (hotspots and hot moments) in denitrification models. *Biogeochemistry*, *93*, 49-77.

11. Illinois-Climate-Network. (2017). Water and atmospheric resources monitoring program. *Illinois State Water Survey, Champaign, Illinois*.

12. Kravchenko, A. N., & Robertson, G. P. (2015). Statistical challenges in analyses of chamber-based soil CO2 and N2O emissions data. *Soil Science Society of America Journal*, *79*(1), 200-211.

13. Kostyanovsky, K. I., Huggins, D. R., Stockle, C. O., Morrow, J. G., & Madsen, I. J. (2019). Emissions of N2O and CO2 following short-term water and N fertilization events in wheat-based cropping systems. *Frontiers in Ecology and Evolution*, *7*, 63.

14. Lawrence, N. C., Tenesaca, C. G., VanLoocke, A., & Hall, S. J. (2021). Nitrous oxide emissions from agricultural soils challenge climate sustainability in the US Corn Belt. *Proceedings of the National Academy of Sciences*, *118*(46), e2112108118.

15. Li, M., Shimizu, M., & Hatano, R. (2015). Evaluation of N2O and CO2 hot moments in managed grassland and cornfield, southern Hokkaido, Japan. *Catena*, *133*, 1-13.

16. Liptzin, D., Silver, W. L., & Detto, M. (2011). Temporal dynamics in soil oxygen and greenhouse gases in two humid tropical forests. *Ecosystems*, *14*, 171-182.

17. Mander, Ü., Krasnova, A., Escuer-Gatius, J., Espenberg, M., Schindler, T., Machacova, K., ... & Soosaar, K. (2021). Forest canopy mitigates soil N2O emission during hot moments. *npj climate and atmospheric science*, *4*(1), 39.

18. Midwestern Regional Climate Center. (2023). *Sub-daily Data Lister*. Retrieved from / /CLIMATE/Hourly/StnHourBTD.jsp.

19. Molodovskaya, M., Singurindy, O., Richards, B. K., Warland, J., Johnson, M. S., & Steenhuis, T. S. (2012). Temporal variability of nitrous oxide from fertilized croplands: hot moment analysis. *Soil Science Society of America Journal*, *76*(5), 1728-1740.

20. Myrgiotis, V., Williams, M., Topp, C. F., & Rees, R. M. (2018). Improving model prediction of soil N2O emissions through Bayesian calibration. *Science of the total environment*, *624*, 1467-1477.

21. Rautakoski, H., Korkiakoski, M., Mäkelä, J., Koskinen, M., Minkkinen, K., Aurela, M., ... & Lohila, A. (2023). Exploring temporal and spatial variation of nitrous oxide flux using several years of peatland forest automatic chamber data. *EGUsphere*, *2023*, 1-34.

22. Risk, N., Snider, D., & Wagner-Riddle, C. (2013). Mechanisms leading to enhanced soil nitrous oxide fluxes induced by freeze–thaw cycles. *Canadian Journal of Soil Science*, *93*(4), 401-414.

23. Roy, A. K., Wagner-Riddle, C., Deen, B., Lauzon, J., & Bruulsema, T. (2014). Nitrogen application rate, timing and history effects on nitrous oxide emissions from corn (Zea mays L.). *Canadian Journal of Soil Science*, *94*(4), 563-573.

24. Saha, D., Kemanian, A. R., Montes, F., Gall, H., Adler, P. R., & Rau, B. M. (2018). Lorenz curve and Gini coefficient reveal hot spots and hot moments for nitrous oxide emissions. *Journal of Geophysical Research: Biogeosciences*, *123*(1), 193-206.

25. Saha, D., Kemanian, A. R., Rau, B. M., Adler, P. R., & Montes, F. (2017). Designing efficient nitrous oxide sampling strategies in agroecosystems using simulation models. *Atmospheric Environment*, *155*, 189-198.

26. Sihi, D., Davidson, E. A., Savage, K. E., & Liang, D. (2020). Simultaneous numerical representation of soil microsite production and consumption of carbon dioxide, methane, and nitrous oxide using probability distribution functions. *Global Change Biology*, *26*(1), 200-218.

27. Soil Survey Staff, Natural Resources Conservation Service, United States Department of Agriculture. Official Soil Series Descriptions. Available online. Accessed [11/03/2023].

28. Song, X., Wei, H., Rees, R. M., & Ju, X. (2022). Soil oxygen depletion and corresponding nitrous oxide production at hot moments in an agricultural soil. *Environmental Pollution*, *292*, 118345.

29. Tallec, T., Brut, A., Joly, L., Dumelié, N., Serça, D., Mordelet, P., ... & Le Dantec, V. (2019). N2O flux measurements over an irrigated maize crop: A comparison of three methods. Agricultural and Forest Meteorology, 264, 56-72.

30. Van den Heuvel, R. N., Hefting, M. M., Tan, N. C. G., Jetten, M. S. M., & Verhoeven, J. T. A. (2009). N2O emission hotspots at different spatial scales and governing factors for small scale hotspots. *Science of the Total Environment*, *407*(7), 2325-2332.

31. Vargas, R., Sánchez-Cañete P, E., Serrano-Ortiz, P., Curiel Yuste, J., Domingo, F., López-Ballesteros, A., & Oyonarte, C. (2018). Hot-moments of soil CO2 efflux in a water-limited grassland. *Soil Systems*, *2*(3), 47.

32. Wagner-Riddle, C., Congreves, K. A., Abalos, D., Berg, A. A., Brown, S. E., Ambadan, J. T., ... & Tenuta, M. (2017). Globally important nitrous oxide emissions from croplands induced by freeze–thaw cycles. *Nature Geoscience*, *10*(4), 279-283.

33. Wagner-Riddle, C., Baggs, E. M., Clough, T. J., Fuchs, K., & Petersen, S. O. (2020). Mitigation of nitrous oxide emissions in the context of nitrogen loss reduction from agroecosystems: managing hot spots and hot moments. *Current Opinion in Environmental Sustainability*, *47*, 46-53.

34. Zhang, Z., Eddy, W. C., Stuchiner, E., DeLucia, E. H., & Yang, W. H. (2023). A new conceptual framework explaining spatial variation in soil nitrous oxide emissions. *bioRxiv*, 2023-11.